Fear Learning Enhances Neural Responses to Threat-Predictive Sensory Stimuli

Marley D. Kass[#], **Michelle C. Rosenthal**[#], **Joseph Pottackal**, and **John P. McGann**[*]
Behavioral and Systems Neuroscience Section, Department of Psychology, Rutgers, The State University of New Jersey, 152 Frelinghuysen Road, Piscataway, NJ 08854

[#] These authors contributed equally to this work.

Abstract

The central nervous system rapidly learns that particular stimuli predict imminent danger. This learning is thought to involve associations between neutral and harmful stimuli in cortical and limbic brain regions, though associative neuroplasticity in sensory structures is increasingly appreciated. We observed the synaptic output of olfactory sensory neurons (OSNs) in individual mice before and after they learned that a particular odor indicated an impending footshock. OSNs are the first cells in the olfactory system, physically contacting the odor molecules in the nose and projecting their axons to the brain's olfactory bulb. Surprisingly, OSN output evoked by the shock-predictive odor was selectively facilitated after fear conditioning. These results indicate that affective information about stimuli can be encoded in their very earliest representations in the nervous system.

Associative learning can alter cortical and even pre-cortical processing in mammalian sensory systems (1-5). However, the primary sensory input is generally thought to be determined by the physical stimulus itself, independent of any prior information the subject may have learned about that stimulus. The development of stably expressed optical activity indicators in mice now permits longitudinal experiments testing whether sensory inputs to the brain remain constant as an individual mouse learns about specific sensory stimuli.

Associative fear conditioning, in which an animal learns that a neutral sensory stimulus predicts the occurrence of an aversive stimulus, can alter the processing of threat-predictive sensory stimuli (6-8). In the olfactory system, fear learning has been shown to enhance difficult olfactory discriminations (9) and alter odorant-evoked neural activity in the piriform cortex and olfactory bulb (9, 10). We used a trial-based, discriminative olfactory fear conditioning paradigm consisting of Paired, Shock Alone Control, and Odor Alone Control groups that underwent either repeated *in vivo* optical imaging procedures or behavioral testing (Fig. 1A). During each of 3 consecutive days of training, mice assigned to the paired group received 5 ~15-sec presentations of each of 2 odorants, one of which (the CS$^+$) always co-terminated with a footshock (Fig. 1B) and one of which (the CS$^-$) did not. Shock-alone and odor-alone groups underwent identical paradigms but without the odor or shock presentations, respectively. When tested in a novel context, mice in the paired group

[*]To whom correspondence should be addressed. jmcgann@rci.rutgers.edu.

exhibited preferential freezing to the CS^+ compared to the CS^-, with comparatively little freezing observed in the shock- or odor-alone control groups, or to a clean air control stimulus (Fig. 1C).

For optical imaging, we used a line of gene-targeted mice that express the fluorescent exocytosis indicator synaptopHluorin (spH) under the control of the olfactory marker protein (OMP) promoter (11), resulting in spH expression in all mature olfactory sensory neurons (OSNs). Odorant-evoked spH signals, indicating neurotransmitter release from OSN terminals into olfactory bulb glomeruli, were visualized *in vivo* using wide-field fluorescence imaging through an implanted cranial window (12, 13) before and after behavioral training (Fig. 1A). Olfactory fear conditioning induced a robust increase in the magnitude of spH responses evoked by the CS^+ odorant compared to pre-conditioning baseline, while no changes were observed in the spH responses evoked by the CS^- or 3 non-presented control odorants (Fig. 2A, 2D-G and 2K). Odorant-evoked spH signals did not differ across imaging sessions in the shock- and odor-alone control groups (Fig. 2B-D and 2H-K). Identical results were obtained regardless of whether glomerular responses were pooled across mice (Fig. 2) or averaged within each individual mouse (Fig. S1). While fear learning augmented CS^+-evoked spH signals, there was no change in the spatial arrangement of CS^+-evoked glomerular response maps (Fig. S2). In a parallel control experiment, no changes in respiration were observed during CS^+ and CS^- presentations in identically-anesthetized, fear conditioned mice (Fig. S3).

Each OSN in the mouse olfactory epithelium expresses one out of hundreds of odor receptor types (14). As OSN axons project ipsilaterally to the olfactory bulb, they segregate by receptor type so that each glomerulus receives projections exclusively from OSNs expressing a specific odor receptor (15). Odorants bind to a subset of olfactory receptor types in the epithelium and thus drive OSN synaptic output into a corresponding subset of olfactory bulb glomeruli. Consequently, the global configuration of odorant-evoked OSN input to glomeruli across the bulb represents the chemical identity of that odorant (16, 17). Because the CS^+ and CS^- were both esters, they drove OSN input to distinct but overlapping populations of glomeruli, reflecting their excitation of partially overlapping populations of OSNs. Some glomeruli selectively received OSN output evoked by the CS^+, while others were selective for the CS^-, and some responded to both odorants (dual-responsive). Separating the odorant-evoked OSN synaptic output based on the odorant-selectivity of each glomerulus revealed that the OSN input to CS^+-selective glomeruli was greatly enhanced, whereas OSN input to glomeruli selective for the CS^- was unchanged (Fig. 3A-B). In dual-responsive glomeruli, there was a selective enhancement when the OSN glomerular inputs were evoked by the CS^+, but *not* when they were evoked by the CS^- (Fig. 3A-B). This differential enhancement was not attributable to scattered light from the responses of CS^+-selective glomeruli (Fig. S4).

The selective enhancement of CS^+-evoked OSN synaptic output in glomeruli whose OSNs are driven by both the CS^+ and the CS^- was unexpected. This discrimination presumably requires that information about the activity of other OSN populations reaches the dual-responsive OSNs to modulate their output. Because this could require feedback from other brain regions, we separated the spH signals into 4, 1-sec time bins (Fig. S5) and tested

whether the degree of enhancement varies across the duration of the odorant presentation. We observed the CS^+-specific enhancement of OSN output not only at the peak of the spH response, but also in constant proportion throughout the entire odorant presentation (Fig. 3C-D and Figs. S5 and S6). No changes were observed for CS^--evoked synaptic input to CS^--selective or dual-responsive glomeruli (Fig. 3C-D and Fig. S6), nor were they observed for time-binned shock- or odor-alone control data (Fig. S7).

Fear conditioning with acetophenone increases the number of OSNs expressing its cognate M71 odorant receptor, and consequently increases the cross-sectional area of their target glomeruli when observed 3 weeks later (18). However, after fear conditioning we did not observe a change in the cross-sectional area of OSN output signals from CS^+-selective, CS^--selective, or dual-responsive glomeruli (Fig. 3E), or in the distributions of glomeruli among these selectivity categories (Fig. 3F). Moreover, the present results cannot be explained by changes in OSN number because an increase in the number of cells in OSN populations excited by both the CS^+ and the CS^- would not selectively facilitate the response of that population to the CS^+ (Fig. 3B). In addition, only 3 days elapsed between fear conditioning and imaging (Fig. 1A), which is less than the 7 days required for newborn OSNs to mature and express OMP ((19); whose promoter drives spH expression in these mice). It is also insufficient time for enhanced survival of mature CS^+-responsive OSNs (which typically survive for months; (20)) to disproportionately increase their numbers. The locus of plasticity may thus lie in the glomerular circuit that presynaptically modulates OSN output (21), instead of in changes in the population of OSNs.

Fear learning enhanced CS^+-evoked OSN output on average across glomeruli (Fig. 2 and Fig. 3A-D), but in fact each mouse receives OSN input to many glomeruli at once. For each mouse, we thus quantified the differences in the overall patterns of OSN input evoked by the CS^+, CS^-, and an unexposed ester both before and after fear learning. The differences (quantified as Euclidean distances in vector space) between the primary sensory representations for the CS^+ and CS^- and between the CS^+ and an unexposed odorant were increased by fear learning (Fig. 3G and Fig. S8). When calculated as a function of time, the fear conditioning-induced difference in representations (presumably predictive of odor discriminability; (17)) was most pronounced during the first second of the stimulus presentations (Fig. 3H and Fig. S8).

Olfactory stimuli typically do not include sharp onsets and offsets. Instead, their concentration varies over time and with distance from the source. OSN firing frequency increases with higher odorant concentrations (22), resulting in more neurotransmitter release from axon terminals into olfactory bulb glomeruli (11). It is possible that the CS^+-selective enhancement of OSN output after fear conditioning is concentration-dependent, such that only OSN responses above some threshold evoke the enhancement. Alternatively, the augmented response to the CS^+ could be concentration-independent, thus enhancing sensitivity to the threat-predictive odorant. We tested these possibilities by presenting the CS^+ and CS^- odorants at 3 different concentrations, including the training concentration (Fig. 1B), half, and double that concentration, during both imaging sessions.

During baseline imaging, the size of the peak spH signals increased as a function of concentration (Fig. 4A-C). Following fear conditioning, CS^+-evoked OSN output was enhanced at all 3 concentrations (Fig. 4A and 4C-D), while CS^--evoked OSN output was unchanged (Fig. 4B-C and 4E). The magnitude of spH signals stimulated by the training CS^+ concentration (Fig. 4D and 4F) was ~68% larger than before conditioning, comparable to the increase at the lower (~73% larger) and higher (~78% larger) concentrations. Similar results were obtained when concentration-response functions were measured earlier in the odorant presentation (Fig. S9). No differences were observed in the concentration-response functions that were evoked by the CS^- (99.6% of baseline; Fig. 4E-F) or in shock- or odor-alone control groups (Fig. S10). Notably, after conditioning, the OSN output that was evoked by the lowest concentration of the CS^+ odorant (4 a.u.) was equivalent to the OSN output evoked by the highest concentration of that odorant (16 a.u.) before conditioning. This suggests that the effect of fear conditioning on OSN output was comparable to the effect of quadrupling the odorant concentration (Fig. 4D and Fig. S9).

These data demonstrate that fear learning can change the neural representation of threat-predictive odors at the synaptic output of the OSNs, which provide the primary olfactory input to the brain. This plasticity may serve to enhance the system's sensitivity to odors associated with an aversive event, perhaps by initiating a large "alarm signal" specific to the CS^+. Such an enhancement could potentially underlie sensory symptoms of anxiety and affective disorders (23), including attentional bias or even PTSD-like hallucinations (6, 24).

Supplementary Material

Refer to Web version on PubMed Central for supplementary material.

Acknowledgments

References and Notes

1. Chen CF, Barnes DC, Wilson DA. J. Neurophysiol. 2011; 106:3136–3144. [PubMed: 21918001]

2. Doucette W, et al. Neuron. 2011; 69:1176–1187. [PubMed: 21435561]

3. Edeline JM, Weinberger NM. Behav. Neurosci. 1991; 105:618–639. [PubMed: 1815615]

4. Gdalyahu A, et al. Neuron. 2012; 75:121–132. [PubMed: 22794266]

5. Kay LM, Laurent G. Nat. Neurosci. 1999; 2:1003–1009. [PubMed: 10526340]

6. Barrett LF, Bar M. Philos. Trans. R. Soc. Lond. B Biol. Sci. 2009; 364:1325–1334. [PubMed: 19528014]

7. Krusemark EA, Li W. J Neurosci. 2013; 33:587–594. [PubMed: 23303938]

8. Headley DB, Weinberger NM. J. Neurosci. 2013; 33:5705–5717. [PubMed: 23536084]

9. Li W, Howard JD, Parrish TB, Gottfried JA. Science. 2008; 319:1842–1845. [PubMed: 18369149]

10. Fletcher ML. Front. Syst. Neurosci. 2012; 6:16. [PubMed: 22461771]

11. Bozza T, McGann JP, Mombaerts P, Wachowiak M. Neuron. 2004; 42:9–21. [PubMed: 15066261]

12. Czarnecki LA, et al. Toxicol. Sci. 2012; 126:534–544. [PubMed: 22287023]

13. Kass MD, Moberly AH, Rosenthal MC, Guang SA, McGann JP. J. Neurosci. 2013; 33:6594–6602. [PubMed: 23575856]

14. Buck L, Axel R. Cell. 1991; 65:175–187. [PubMed: 1840504]

15. Mombaerts P, et al. Cell. 1996; 87:675–686. [PubMed: 8929536]

16. Malnic B, Hirono J, Sato T, Buck LB. Cell. 1999; 96:713–723. [PubMed: 10089886]

17. Youngentob SL, Johnson BA, Leon M, Sheehe PR, Kent PF. Behav. Neurosci. 2006; 120:1337–1345. [PubMed: 17201479]

18. Jones SV, Choi DC, Davis M, Ressler KJ. J. Neurosci. 2008; 28:13106–13111. [PubMed: 19052201]

19. Miragall F, Monti Graziadei GA. Brain Res. 1982; 239:245–250. [PubMed: 7046875]

20. Carr VM, Farbman AI. Exp. Neurol. 1993; 124:308–314. [PubMed: 8287929]

21. McGann JP. Chem. Senses. 2013; 38:459–474. [PubMed: 23761680]

22. Reisert J, Matthews HR. J. Physiol. 2001; 530:113–122. [PubMed: 11136863]

23. Beck AT, Clark DA. Behav. Res. Ther. 1997; 35:49–58. [PubMed: 9009043]

24. Felmingham KL, Rennie C, Gordon E, Bryant RA. Biol. Psychol. 2012; 90:224–227. [PubMed: 22476033]

25. Czarnecki LA, et al. Neurotoxicology. 2011; 32:441–449. [PubMed: 21443902]

26. Kass MD, Moberly AH, McGann JP. PLoS One. 2013; 8:e61431. [PubMed: 23630588]

27. Ottoni EB. Behav. Res. Methods. Instrum. Comput. 2000; 32:446–449. [PubMed: 11029818]

28. Kass MD, Pottackal J, Turkel DJ, McGann JP. Chem. Senses. 2013; 38:77–89. [PubMed: 23125347]
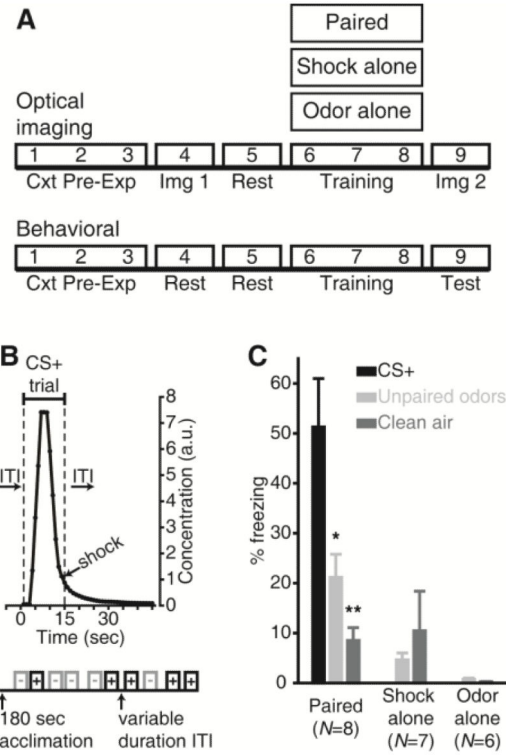
Fig. 1.
Olfactory fear learning and conditioned freezing. (**A**) Timeline of experiments. Cxt Pre-Exp, context pre-exposure; Img, imaging. (**B**) Protocol summary for 1 day of Paired training, with expanded CS^+ trial showing the delivery of odorant (arbitrary units, a.u.) and shock stimuli. (**C**) Mean±SEM percent time freezing during the behavioral test session. *$P < 0.05$, **$P < 0.01$ by Bonferroni-corrected *post-hoc* comparisons; *N*, mice/group.
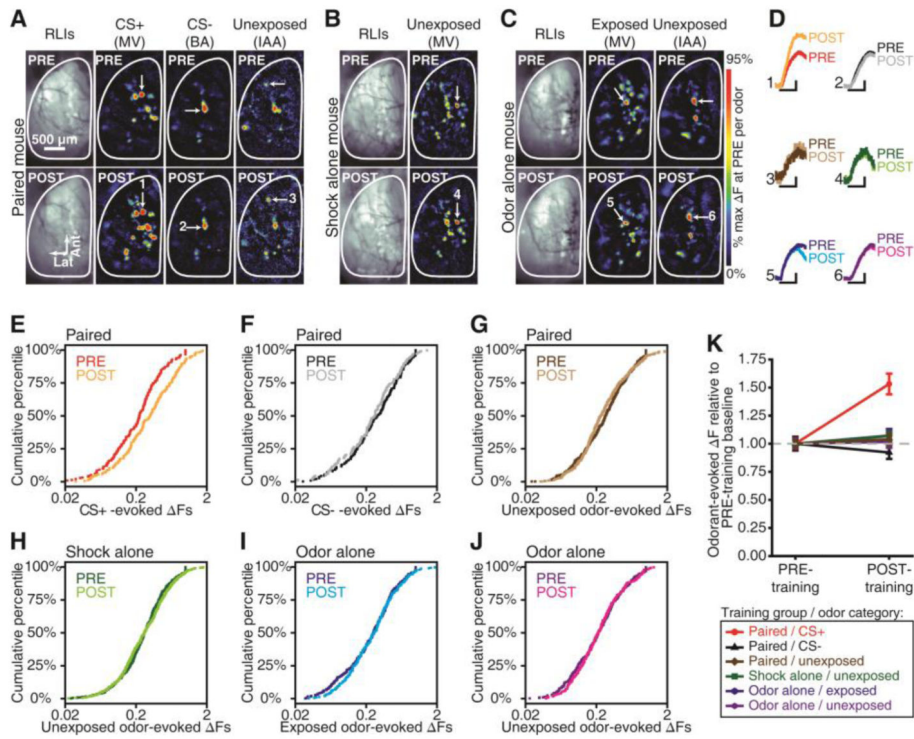
Fig. 2.

Fear learning-induced plasticity in odorant-evoked nerve output. **(A-C)** PRE vs. POST resting light images (RLIs) and pseudocolored difference maps from representative fear conditioned **(A)**, shock alone **(B)**, and odor alone **(C)** mice. MV, methyl valerate; BA, butyl acetate; IAA, isoamyl acetate. **(D)** Odorant-evoked change in fluorescence (ΔF) corresponding to callouts in **A-C**. Scale bars, 6-sec stimulus, 25% max of PRE. **(E-J)** Cumulative probability plots showing the distributions of PRE vs. POST ΔF values that were evoked by the CS^+ (**E**; $P \leq 0.001$), CS^- (**F**; $P > 0.05$), and all other unexposed odorants (**G**; $P > 0.05$) in the paired group, all unexposed odorants in the shock alone group (**H**; $P > 0.05$), and all exposed (**I**; $P > 0.05$) and unexposed (**J**; $P > 0.05$) odorants in the odor alone group. P values are by K-S tests. **(K)** Mean±SEM ΔF pooled across glomeruli (dashed line, baseline). Number (N) of glomeruli contributing to data in **E-K**: paired, $N_{PRE} = 267$, $N_{POST} = 285$; shock alone, $N_{PRE} = 163$, $N_{POST} = 173$; odor alone, $N_{PRE} = 209$, $N_{POST} = 180$.
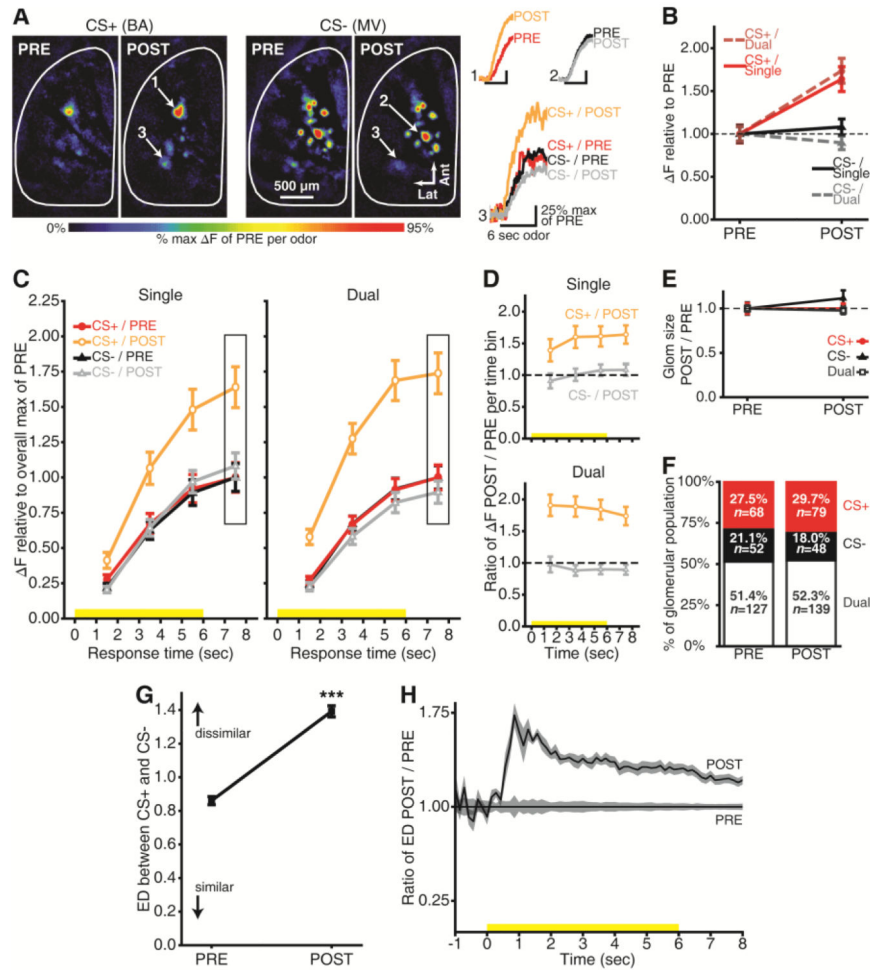
Fig. 3.
Stimulus-specific enhancement of nerve output. **(A)** PRE vs. POST CS$^+$- and CS$^-$-evoked maps from a representative mouse. Numbered callouts show example traces from single- and dual -responsive glomeruli. Butyl acetate, BA; methyl valerate, MV. **(B)** Peak odorant-evoked change in fluorescence (F) separated by selectivity (dashed line, baseline). **(C)** Time-binned odorant-evoked F for single- and dual-responsive glomeruli. Boxed regions indicate the bin corresponding to peak responses in **A-B**. Yellow stimulus bars show odorant presentations. **(D)** Ratio of CS$^+$ and CS$^-$-evoked Fs during POST / PRE per bin per selectivity category (dashed line, baseline). **(E)** Glomerulus response size shown relative to PRE (dashed line). **(F)** Percent of PRE- and POST-training glomerular populations per selectivity category. $P > 0.05$, by χ^2; Ns, number of glomeruli contributing to means±SEM in **B-E**. **(G-H)** Example network-level analysis from one mouse. **(G)** PRE vs. POST mean±SEM Euclidean distance (ED) between CS$^+$- and CS$^-$-evoked maps pooled across trial pairs and response times (0-8 sec). ***$P < 0.001$ by factorial ANOVA. **(H)** Proportional increase in dissimilarity between odor representations as a function of time. Solid lines ±shading, mean±SEM.
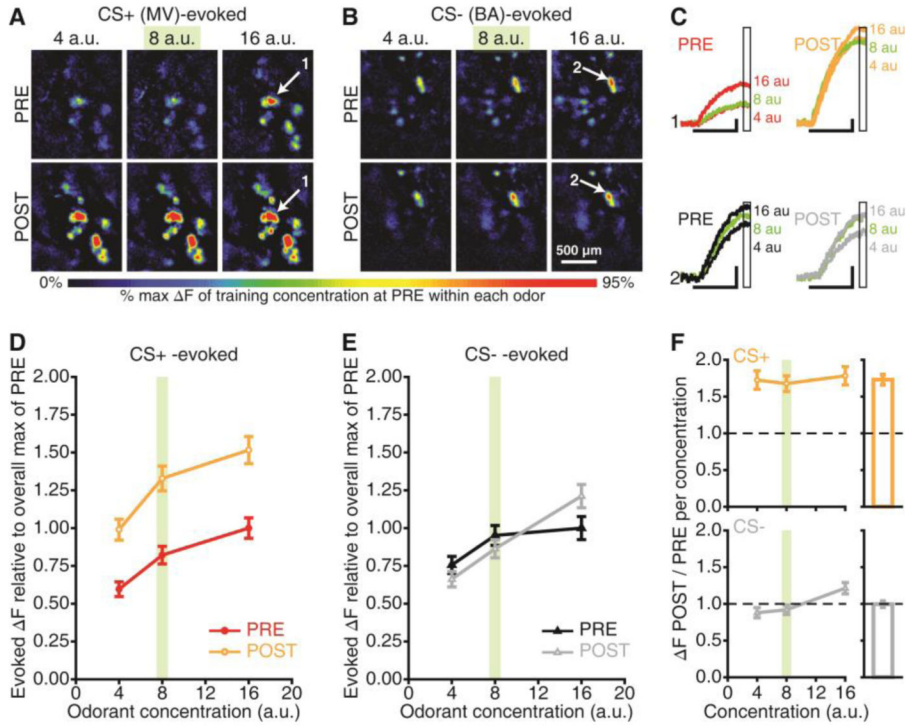
Fig. 4.
Enhanced sensitivity to the CS[+]. **(A-B)** Maps evoked by 3 concentrations (arbitrary units, a.u.) of the CS[+] and CS[−] before and after this mouse underwent fear conditioning. MV, methyl valerate; BA, butyl acetate. **(C)** Response amplitudes (Fs) for callouts **(A-B)**. Scale bars, 6-sec stimulus, 25% max of PRE. Boxed regions indicate the bin used to generate peak maps **(A-B)** and concentration analyses **(D-F)**. **(D-E)** PRE vs. POST CS[+]- and CS[−]-evoked concentration-response functions. **(F)** Ratio of CS[+]- and CS[−]-evoked Fs during POST / PRE per concentration (dashed lines, baseline). Outsets are scaled to the main *y*-axis and show overall ratios pooled across concentrations. Data are pooled across glomeruli (mean±SEM) in **D-F**. The training concentration is indicated in green in **A-F**.